Evaluation and comparison of colorimetric outputs for yeast-based biosensors in laboratory and point-of-use settings

FEMS Microbiology Letters, 2024, **371**, fnae034
DOI: 10.1093/femsle/fnae034
Advance access publication date: 23 May 2024
Research Letter – Biotechnology & Synthetic Biology

Evaluation and comparison of colorimetric outputs for yeast-based biosensors in laboratory and point-of-use settings

Andrea Clausen Lind [1], Florian David[1], Verena Siewers[1,2,*]

[1]Department of Life Sciences, Chalmers University of Technology, 412 58 Gothenburg, Sweden
[2]Novo Nordisk Foundation Center for Biosustainability, Technical University of Denmark, DK-2800 Kgs. Lyngby, Denmark
*Corresponding author. Department of Life Sciences, Division of Systems and Synthetic Biology, Chalmers University of Technology, Gothenburg SE-41296, Sweden. E-mail: siewers@chalmers.se
Editor: [Matthias Steiger]

Abstract

Recent research has shown the potential of yeast-based biosensors (YBBs) for point-of-use detection of pathogens and target molecules in saliva, blood, and urine samples. The choice of output can greatly affect the sensitivity, dynamic range, detection time, and ease-of-use of a sensor. For visual detection without the need for additional reagents or machinery, colorimetric outputs have shown great potential. Here, we evaluated the inducible generation of prodeoxyviolacein and proviolacein as colorimetric YBB outputs and benchmarked these against lycopene. The outputs were induced via the yeast mating pathway and were compared on agar plates, in liquid culture, and on paper slips. We found that all three outputs produced comparable pigment intensity on agar plates, making them applicable for bioengineering settings. In liquid media and on paper slips, lycopene resulted in a higher intensity pigment and a decreased time-of-detection.

Keywords: biosensors; GPCR; colorimetric outputs; point-of-care detection; yeast mating pathway

Introduction

Yeast-based biosensors (YBBs), utilizing *Saccharomyces cerevisiae* as a chassis for detection of a target molecule, have been developed for a wide array of applications. Looking at the current scope of developed YBBs, these largely target industrial, pharmacological research and bioengineering applications (Adeniran et al. 2015, Jarque et al. 2016, Wahid et al. 2023). In these areas, YBBs are utilized for a wide array of sensing tasks, e.g. quantification of valuable compounds (Miettinen et al. 2022), characterization of orphan receptors and synthetic ligands (Kapolka et al. 2020), and screening of strain libraries (Skrekas et al. 2022). In recent years, the potential of YBBs for applications outside of laboratory settings has been revealed through development of YBBs for on-site detection of e.g. pathogenic fungi (Ostrov et al. 2017) and (-)-trans-Δ9-tetrahydrocannabinol (THC) (Miettinen et al. 2022) in complex samples such as soil, saliva, blood, urine, and serum. Owing to the low cost of production of YBBs and their stability at room-temperature, YBBs show great potential as an alternative to the commonly used protein-based sensors (Adeniran et al. 2015). To be applicable on-site, the output signal of the YBB needs to be clear and readable in absence of special equipment, while providing a rapid and reliable response. High sensitivity, specificity, dynamic range, and a short time-of-detection (TOD) are thus key biosensor properties, which are affected by the choice of output (Lopreside et al. 2019). Here, we aim to evaluate the applicability of two colorimetric outputs, prodeoxyviolacein and proviolacein, for biosensor deployment in both bioengineering and non-laboratory settings, and to benchmark these against the previously established lycopene output (Ostrov et al. 2017).

There are two main types of YBBs, i.e. transcription-independent and transcription-dependent sensors. While transcription-independent sensors utilize already existing components within the cell to form an output signal in presence of the target compound, transcription-dependent sensors rely on transcriptional activation in response to the ligand and subsequent synthesis of proteins conferring a response (Adeniran et al. 2015). For detection of low concentrations of a target molecule, transcription-dependent sensors are often advantageous as these allow for signal amplification, generating several transcripts of the output protein per molecule detected. In this work, we utilize a transcription-dependent system based on a streamlined pheromone sensing pathway in yeast (Fig. 1A) (Shaw et al. 2019), as a platform for benchmarking of the colorimetric outputs.

The mating pathway of yeast is activated through the binding of a mating pheromone from the opposite mating type (a/α) to the cognate mating G-protein coupled receptor (GPCR; Ste3/Ste2). The binding induces a conformational change of the GPCR resulting in exchange of GDP to GTP in the associated heterotrimeric G-protein Gα subunit (Gpa1), and in turn dissociation of Gα from the G$\beta\gamma$-complex (Ste4-Ste18) (Fig. 1A) (Bardwell 2005). Subsequently, the G$\beta\gamma$ dimer activates a mitogen-activated protein kinase (MAPK) cascade resulting in activation of the transcription factor (TF) Ste12 ultimately triggering the mating response through transcription activation of mating-related genes (Fig. 1A)

Received 27 February 2024; **revised** 30 April 2024; **accepted** 22 May 2024

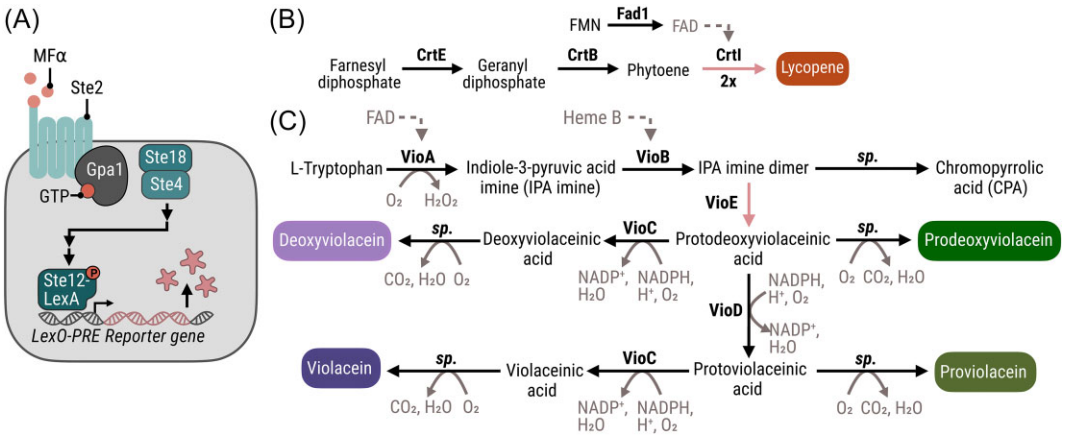

Figure 1. Strain design and biosynthetic pathways. (A) Minimized *S. cerevisiae* mating pathway, engineered for a linear response with low background expression based on previous work by Shaw and colleagues, but in the CEN.PK strain background (Shaw et al. 2019). Only the central pathway components for which expression levels were modified (*STE2*, *GPA1*, *STE12-LexA*, reporter gene) are depicted. The binding domain of TF Ste12 was replaced with that of LexA, enabling use of a synthetic inducible promoter (LexO-PRE) for reporter gene expression. (B) Biosynthetic pathway of the colorimetric output lycopene (red). Two copies of the gene 4. encoding CrtI were expressed under the synthetic promoter. CrtE, geranylgeranyl diphosphate synthase; CrtB, phytoene synthase; CrtI, phytoene desaturase; Fad1, flavin adenine dinucleotide synthase; FMN, farnesyl mononucleotide; FAD, flavin adenine dinucleotide. (C) Overview of the violacein pathway and colorimetric products prodeoxyviolacein (green), proviolacein (brown/green), deoxyviolacein (purple), violacein (dark purple), and side product chromopyrrolic acid (CPA). For production of prodeoxyviolacein, VioA-B and VioE were expressed, and for the production of deoxyiolacein VioA-B and VioD-E were expressed. In both strains, VioE was expressed under the synthetic promoter. VioA, flavin-dependent L-tryptophan oxidase; VioB, 2-imino-3-(indol-3-yl)propanoate dimerase; VioC, violacein synthase; VioD, protodeoxyviolaceinate monooxygenase; VioE, violacein biosynthesis enzyme; *sp*., spontaneous.

(Bardwell 2005). By replacing the mating response genes with those generating an output of choice, one can thus produce an alternative response such as formation of a pigment (Ostrov et al. 2017). Additional replacement of Ste2 with a GPCR of choice enables cell-surface based detection of a wide array of extracellular compounds and does not require ligands to cross the cell membrane, as is needed for transcription-factor-based sensors (Adeniran et al. 2015). This is highly applicable for development of sensors to be used in clinical and industrial settings, where target ligands may not be able to enter the cell.

Different outputs have been coupled to the yeast mating pathway depending on the target application, such as expression of fluorescent proteins (Shaw et al. 2019, Kapolka et al. 2020), luciferase enzyme enabling bioluminescence (Miettinen et al. 2022), and enzymes creating colorimetric outputs (Ostrov et al. 2017). Of these, colorimetric and bioluminescent outputs are both detectable in the absence of additional equipment, but while bioluminescence formation often requires addition of external reagents (Miettinen et al. 2022), colorimetric outputs usually do not (DeLoache et al. 2016, Ostrov et al. 2017). The choice of output can heavily affect the TOD of a mating-pathway based YBB (Miettinen et al. 2022). Bioluminescence output resulted in the shortest TOD, about 30 min after induction. However, the ease-of-use for this output is reduced and the cost is increased as it requires both cell lysis and external reagents, in addition to a camera attachment for light-free imaging (Miettinen et al. 2022). Meanwhile, colorimetric outputs enable detection by the naked eye without further processing of the cells. The red pigment lycopene has been evaluated previously as a YBB output for point-of-care (POC) use, enabling detection by the naked eye within 3 h of induction in liquid and within 8 h on paper slips without addition of external compounds (Ostrov et al. 2017).

Aiming to increase the repertoire of colorimetric outputs for YBB applications, we investigated the green prodeoxyviolacein and green-brown proviolacein pigments as alternative colorimetric YBB outputs and benchmarked these against lycopene. Both compounds produce strong pigments in yeast, and have shown potential as biosensor outputs (DeLoache et al. 2016, Rantasalo et al. 2018, Sanford et al. 2022). Pathway genes of the respective outputs were introduced in the genome of a YBB platform strain, and the outputs were compared in terms of TOD and pigment intensity. To gauge the applicability of the different outputs in bioengineering, industrial, and on-site settings, the outputs were compared in three different conditions: on agar plates to investigate the effect of media complexity on induction of the respective outputs, in liquid culture, and finally on paper slips to investigate applicability of POC testing.

Methods

Strains and growth media

Escherichia coli DH5α was used for plasmid assembly and propagation, cultivated in LB media with kanamycin, ampicillin, or chloramphenicol selection. Details on media preparation can be found in Supplementary Methods.

Saccharomyces cerevisiae strains in this study were derived from IMX581, with a CEN.PK strain background, constructed through iterative rounds transformations using CRISPR/Cas9 for seamless deletions and insertions. Mating pathway genes for which expression levels were modified (*GPA1*, *STE12-LexA*, and *STE2*) and inducible promoter (*pLexO(6x)Leu2*) were amplified form the genome of strain Design 4, developed by Shaw and colleagues in a S288C strain background (Shaw et al. 2019). Genes *crtB, crtB*, and *crtI* of the *Erwinia herbicola* lycopene pathway were retrieved from the article by Ostrov and colleagues in 2017 (Ostrov et al. 2017). Amino acid sequences of violacein pathway genes *vioA*, *vioA*, *vioC*, *vioD*, and *vioE* from *Chromobacterium violaceum* were retrieved from NCBI and the genes were codon optimized for *S. cerevisiae* (see Supplementary Methods for details on strain construction, and find strain specifications, gene sequences, oligos, and plasmids used in this study in Tables S1–S4). YPD medium and synthetic defined (SD) agar plates lacking uracil or supplemented with 5-FOA

were used in strain construction. For evaluation of induction of colorimetric outputs, YPD at pH 5.8, SD complete (SDC) pH 5.8, and SDC with 5% YPD (SDC + 5%YPD) medium mixed from the separately prepared media were used. For induction, 1 μM of *S. cerevisiae* α-mating pheromone (GenScript) was added to the media from a 1000x stock with 10% DMSO and an equal volume of 10% DMSO solution was added to controls. Details on media preparation can be found in Supplementary Methods. All strains used in this study are listed in Table S1.

Colorimetric output evaluation on agar plates

The effect of different media on induction of lycopene, prodeoxyviolacein, and proviolacein production was evaluated on agar plates with three levels of media complexity, with or without addition of 1 μM of the Sc α-mating pheromone. Agar plates were prepared with three media complexities: minimal (SDC), mixed (SDC + 5%YPD) and complex (YPD) in square 120.5 mm petri dishes to which 40 mL of media with agar was added. Output null strain with the Ste2 receptor (AMG0-1), lycopene strains without/with the receptor (AlCG0/AlCG0-1), prodeoxyviolacein strains without/with receptor (APDG0/APDG0-1), and proviolacein strains without/with receptor (APVG0/APVG0-1) were seeded in 5 mL SDC media in 50 mL falcon tubes and incubated 15 h overnight at 30°C and 200 rpm. Part of each culture was pelleted and resuspended to an OD_{600} of 0.5 in 2 mL of SDC, SDC + 5%YPD, and YPD, respectively, in a 12 mL breathing cap tube. Cultures were incubated 5 h at 30°C and 200 rpm. Cells were harvested in the exponential growth phase, pelleted, and the supernatant was removed before resuspension of cells in sterile milliQ water to an OD_{600} of 5. A 10x dilution series in three steps was made for each culture, to gauge the effect of cell density on pigment development. Then 5 μL of each strain and dilution was dropped onto each of the plates corresponding to the preculture medium, preparing plates with and without 1 μM α-pheromone for each medium. Two strain replicates were used, plated on separate plates. Agar plates were incubated at 30°C for 2 weeks, collecting pictures after 24 h, 48 h, 72 h, and 2 weeks.

Photos were taken with an Oneplus Nord 2 mobile camera in Pro mode, with fixed settings. To even-out light conditions across photos and reduce reflection in plate lids, a folding portable photo box (Puluz, PU5021) was used. Red, green, and blue intensities for each spot were extracted in ImageJ, from which the relative red respectively green intensity values were calculated (Ostrov et al. 2017).

Evaluation of lycopene, prodeoxyviolacein, and proviolacein content in liquid cultures

The method used was based on the protocol developed by Ostrov and colleagues for evaluation of intracellular lycopene in a yeast culture (Ostrov et al. 2017). Output strains were evaluated in liquid media to determine the time-of-detection and intensity of each output. Robust and sensitive wavelengths, for collection of pigment independent and dependent measurements, were determined based on the absorbance spectra of induced output strains (AlCG0-1, APDG0-1, APVG0-1) relative to the output null strain (AMG0-1), details in Supplementary Methods. For evaluation of absorbance, strains were seeded in 5 mL SDC + 5%YPD in 50 mL falcon tubes and cultivated for 14 h overnight at 30°C and 200 rpm. Part of cultures were pelleted and resuspended to an OD_{600} of 2 in 3 mL fresh SDC + 5%YPD medium in a 50 mL falcon tube with and without 1 μM α-pheromone. Cultures were incubated at 30°C and 200 rpm. Three replicates were used per strain and condition.

Then, 35 μL was sampled from each culture 0, 1, 2, 3, 4, 6, 10, and 24 h after induction, and was analyzes in a 96-well half-area UV-STAR microplate (Greiner, 675 801). Absorbance was measured in a FLUOstar Omega microplate reader, at the robust and sensitive wavelengths determined for the respective output strains. The plate was set to 10 s shaking at 800 rpm before measurement. Adjustment of absorbance measurements to counter for absorbance saturation caused by high cell densities was attempted in accordance with previous publications (Lin et al. 2010, Ostrov et al. 2017), but was not applied to the final data. Instead, the lycopene, prodeoxyviolacein, and proviolacein absorbance were calculated based on robust and sensitive absorbance measurements (Ostrov et al. 2017), and the relative absorbance compared to the output-null strain was calculated and plotted.

Colorimetric output evaluation on paper slips

Output strains were evaluated on paper slips to determine the time-of-detection and output intensity over time from induction. Output strains with (AlCG0-1, APDG0-1, APVG0-1) and without receptor (AlCG0, APDG0, APVG0) were cultivated in 10 mL YPD in 50-mL falcon tubes at 30°C and 200 rpm for 24 h. Cells were dried onto glass fiber filter paper (Thermo Scientific, DS0281-7500) in a 5 mm in diameter circular area using vacuum filtration and a pipette rack as a scaffold, to a cell count of corresponding to 2.4∗10^6.

For evaluation, output strain pairs with/without the receptor were evaluated side-by-side, by placing 10 × 10 mm square cutouts for each strain on wicking paper (Tork hand paper towel) dipped in media. Two conditions were evaluated, YPD media with or without 1 μM added α- pheromone. Two 48-well plates were used for evaluation, adding 2 mL media to each well and bridging wicking paper between two wells. To prevent evaporation, a lid was placed on the box. Three strain replicates were used. Photos were taken with a Canon DC 8.1 V, using a styrofoam-based photo box built from cuvette boxes in order to soften and even out light from the camera flash. The camera position was fixed in place in the lid of the photo box. ImageJ was used to extract red, green, and blue intensities for each spot, from which the relative red respectively green intensity values were calculated (Ostrov et al. 2017). From these values the difference in output intensity of strains with and without receptor were compared.

Results and discussion

In order to obtain a platform strain for output evaluation with low background expression and a linear response, we opted to utilize the minimal mating pathway developed by Shaw and colleagues (Shaw et al. 2019) (Fig. 1A). While their strain was developed in a S288C strain background, we re-implemented the developed pathway in a CEN.PK strain background due to the wider array of engineering tools available for this strain in our lab (Shaw et al. 2019). The pathway generates an inducible output in response to the α-mating pheromone of *S. cerevisiae*. Pathway components involved in feedback regulation (Sst2, Bar1) and cell-cycle arrest (Far1) were removed to avoid unexpected fluctuations in the induction response. In addition, several genes related to the mating pathway (*MFA1, MFA2, MF(alpha)1, MF(alpha)2, STE3*) and GPCR-based sugar sensing (*GPR1, GPA2*) were deleted (Shaw et al. 2019). Lastly, selected central components of the mating pathway (Ste2, Gpa1, Ste12) were removed, before being re-introduced under control of alternative promoters and terminators (Shaw et al. 2019). In the case of Ste12, this TF was replaced by the synthetic vari-

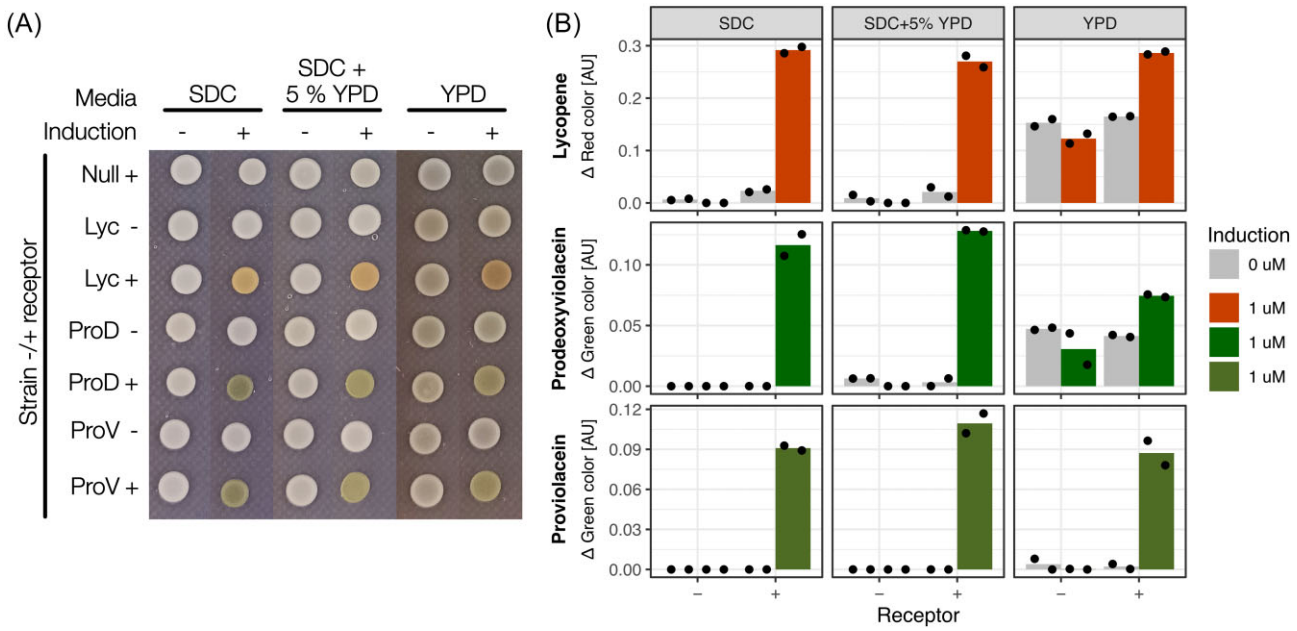

Figure 2. Colorimetric output induction on agar plates. (A) Strains were spotted onto agar plates with minimal (SDC), mixed (SDC + 5%YPD), and high (YPD) medium complexity with (+) or without (-) 1 μM of the *S. cerevisiae* α-mating pheromone. Pictures of plates were taken after 72 h of incubation. (B) Bar plots showing output intensity calculated from pictures of agar plates after 72 h of incubation. Red color intensity was calculated to determine lycopene output and green color intensity to determine proviolacein and prodeoxyviolacein outputs, respectively. To correct for variation in intensity caused from differences in media pigmentation, the pigment intensity was calculated relative to the output null strain on the same agar plate with or without the receptor, respectively. Two strain replicates were evaluated. Negative values were set to zero.

ant Ste12-LexA, binding synthetic promoter pLexO(6x)Leu2, to enable a lower baseline in absence of induction (Shaw et al. 2019). These modifications were implemented in strain IMX581, to produce an output-null control strain with the receptor (AMG0-1), and without receptor (AMG0). Induced genes were expressed under the synthetic promoter pLexO(6x)Leu2. For initial validation of the pathway, we opted to use GFP as an inducible output (AMSG0-1). Evaluating the dose-response for increasing concentrations of α-mating pheromone in SDC media, we found a low baseline expression in our strain, and that the sensor was fully activated at 50 nM and above (Fig. S1A-B). To evaluate the full potential of each pigment, all further evaluation was carried out using 1000 nM α-mating pheromone.

The lycopene expression pathway has previously been optimized for use as an colorimetric output (red) of the yeast mating pathway (Ostrov et al. 2017). Including the *crtI, crtB,* and *ctrE* genes from *Erwinia herbicola*, and the *FAD1* gene from *S. cerevisiae*, with two copies of *crtI* expressed as an inducible output, lycopene is produced from the precursor farnesyl diphosphate (Fig. 1B) (Ostrov et al. 2017). Genes were separated into two integration cassettes, using the inducible promoter for *crtI* expression, and strong constitutive promoters for expression of the remaining genes. Expression cassettes were integrated in the genome of strain of AMG0, resulting in strain AlCG0 without receptor and AlCG0-1 with receptor.

The violacein pathway from *Chromobacterium violaceum* has 4 colorimetric products, including prodeoxyviolacein (green), proviolacein (green/brown), deoxyviolacein (pink/purple), and violacein (dark purple). It consists of five genes, *vioA, vioB, vioC, vioD,* and *vioE*, of which different combinations can be expressed to produce the respective products from L-tryptophan (Fig. 1C) (Lee et al. 2013, DeLoache et al. 2016, Rantasalo et al. 2018). To construct strains expressing prodeoxyviolacein and proviolacein, *vioC* and *vioC-D* respectively were excluded. *VioE* was expressed under the inducible promoter, selected due to the absence of pigment of the precursor. Strong constitutive promoters corresponding to those used for expression of the lycopene pathway were used for the remaining genes. Pathway genes were separated over two expression cassettes and integrated in the genome of strain AMG0, producing the proviolacein strain APVG0 and prodeoxyviolacein strain APDG0 without receptor, and strains APVG0-1 and APDG0-1, respectively, with receptor.

We first evaluated the effects of medium complexity on output induction, as varying media complexities may be required depending on the YBB application. For employment in bioengineering settings, defined media are often preferred, while complex media are commonly applied for clinical and industrial applications. To assess this, we performed a spot-test on agar plates with three levels of medium complexity: minimal (SDC), mixed (SDC + 5%YPD) and complex (YPD). Strains with and without the receptor were evaluated in absence or presence of 1 μM α-pheromone (Fig. 2A). Comparing the red and green pigment intensity for lycopene, prodeoxyviolacein and deoxyviolacein strains, respectively, calculated relative to the output-null strain on the same plate, we found that medium complexity indeed affects the output (Fig. 2B). Each of the colorimetric outputs were clearly detectable by the naked eye after 72 h of incubation independent of the medium (Fig. 2A), with little difference in output intensity between minimal and mixed complexity media (Fig. 2B). Interestingly, we found that for all outputs, incubation on complex medium resulted in an increased baseline expression, identified after 72 h for lycopene and prodeoxyviolacein strains (Fig. 2B) and after a prolonged incubation for the deoxyviolacein strain (Supplementary Figure S2). Note however, that the baseline expression did not impair the readout clarity. While our strain was designed for low basal expression in minimal media, this is obviously something that can be influenced by an altered medium complexity (also relevant for designs developed in

Table 1. The three wavelengths from with the relative pigment absorbance is calculated for each colorimetric output are listed below, and at sensitive wavelengths, the colorimetric output largely contributes to absorbance.

Output	Robust wavelength[a] 1 (nm)	Robust wavelength[a] 2 (nm)	Sensitive wavelength[b] (nm)
Lycopene	395	600	520
Prodeoxyviolacein	395	750	450
Proviolacein	395	750	450

[a]At robust wavelengths, absorbance is unaffected by the colorimetric output.
[b]At sensitive wavelengths, the colorimetric output largely contributes to absorbance.

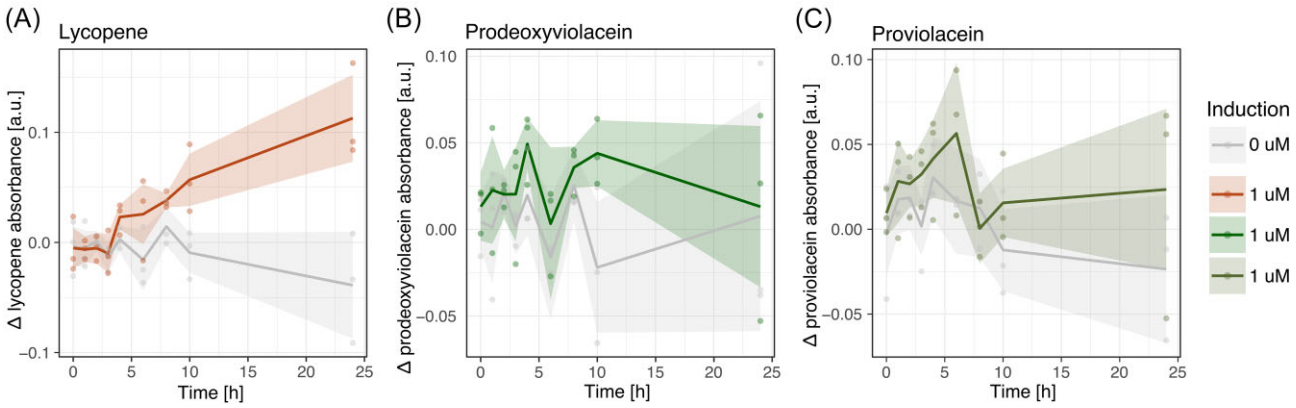

Figure 3. Colorimetric output induction in liquid culture. Colorimetric output production of (A) lycopene, (B) prodeoxyviolacein, and (C) provilolacein over time for strains grown in SDC + 5%YPD media with or without 1 μM *S. cerevisiae* α-mating pheromone. Absorbance at sensitive and robust wavelengths (Table 1) were measured in microplate reader, and the lycopene, prodoxy- and proviolacein levels per cell (not corrected for absorbance saturation) relative to the output null strain were calculated. Solid lines indicate mean across triplicates and shaded regions indicate +/- 1 s.d. from the mean for three strain, while dots indicate values of the single replicates.

complex media) and is important to consider this when designing an YBB.

Unexpectedly, the presence of α-pheromone appears to result in a slight reduction in spot diameter in all strains with the receptor independent of the medium (Fig. 2A). This was also the case for the output-null strain, indicating that allocation of resources towards pigment production or toxicity of the pigment was not the cause of the reduced growth (Fig. 2A). With the removal of Far1, responsible for cell-cycle arrest during mating, and the majority of mating-related genes it is likely that the slight growth impediment is caused by unexpected pathway interactions (Kemp and Sprague 2003, Bardwell 2005, Strickfaden et al. 2007). The combined deletions in the mating pathway may also have had an unexpected effect on genes regulated by the pathway, as several genes are co-regulated by multiple TFs (Esch et al. 2006) (extended discussion in Supplementary Information Note 1). While the majority of evaluations were performed after 72 h of incubation, outputs were already clearly visible independent of the medium after 24 h (Fig. S2).

Next, strains were evaluated in liquid cultures to determine the applicability of the respective outputs for on-site or industrial settings. For analysis we used mixed complexity medium mimicking the higher complexity of clinical samples while minimizing the impact of background absorbance on measurements. We attempted to adapt a method previously used for robust intracellular lycopene quantification for deoxyviolacein and prodeoxyviolacein measurements (Lin et al. 2010, Ostrov et al. 2017). The method utilizes absorbance at three separate wavelengths to calculate the relative content of the respective compounds. Of the three wavelengths, two are robust wavelengths at which the absorbance is unaffected by the pigment absorbance, and one is a sensitive wavelength at which the pigment largely contributes to the absorbance. While this was simple for lycopene, selection of robust and sensitive wavelengths for proviolacein and prodeoxyviolacein was impeded by the weak intensity of the pigments in liquid media (Fig. S3A-B). Based on these absorbance spectra, robust and sensitive wavelengths selected for lycopene, prodeoxyviolacein, and proviolacein (Table 1).

Using the robust and sensitive wavelengths, the absorbance was calculated for the lycopene, prodeoxyviolacein, proviolacein, and output-null strains with receptor. Strains were cultivated in media in the presence or absence of 1 μM α-pheromone and sampled over time to gauge pigment development and intensity. Calculating the relative absorbance compared to the output-null strain for the respective strains and timepoints, we found that the levels of lycopene were measurable after 4 h of induction, while we were not able to detect prodeoxyviolacein or proviolacein using absorbance measurements throughout the 24 h sampling period (Fig. 3A–C).

We were puzzled by the lower intensity of the prodeoxy- and proviolacein pigments in liquid settings compared to induction on agar plates after 24 h. A potential explanation could be different rates of production of the respective pigments (extended discussion in Supplementary Information, Note 2). We additionally considered whether oxygen, required for the spontaneous conversion of precursors into the pigments (Lee et al. 2013), could be limiting. However, this is unlikely to be the case in the given experimental settings. While the implemented lycopene pathway has been optimized for inducible expression in prior work (Ostrov et al. 2017), the implemented violacein pathway has not. Overall, extensive work has been focused on optimization of lycopene production, reporting titers of up to 2.37 g/L over a 5 day fed-batch cultivation

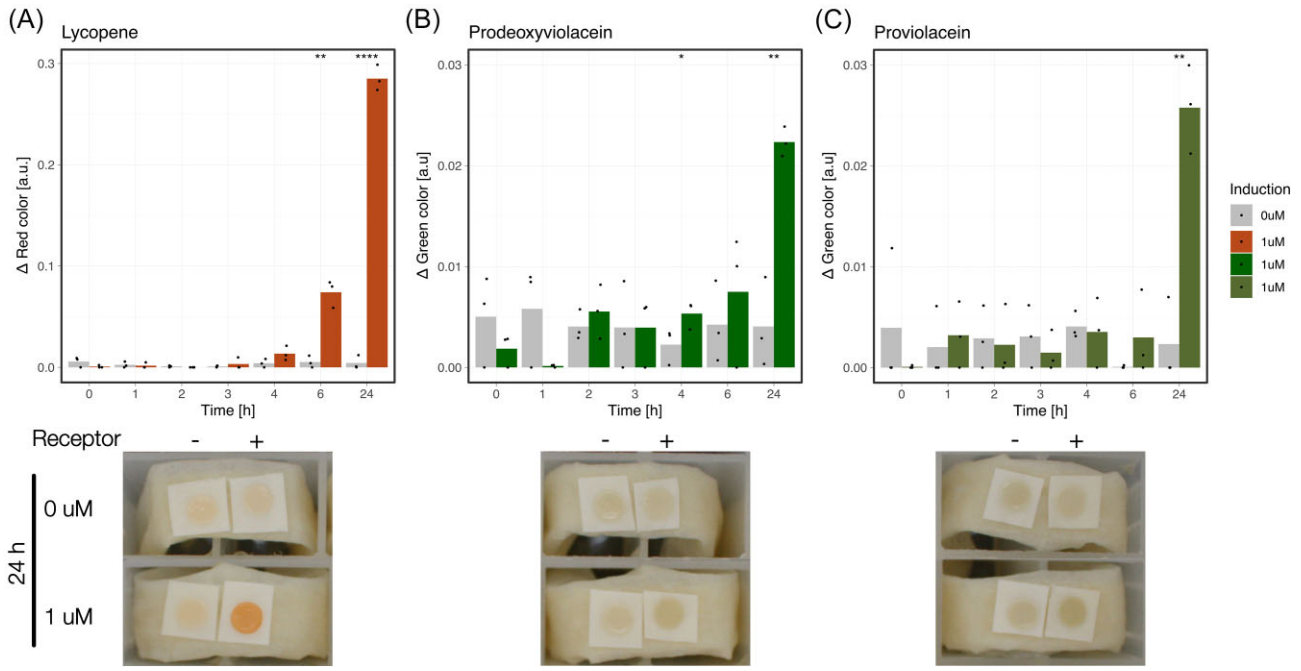

Figure 4. Colorimetric output induction on paper slips. Output strains with (+) or without (−) receptor were dried onto paper slip and placed onto wicking paper dipped in YPD media with 0 μM or 1 μM *Sc* α-mating pheromone. Photos were taken over time to monitor the pigment development and were analyzed in ImageJ to calculate red respectively green pigment. Bar plots show the difference in colorimetric output production of (A) lycopene, (B) prodeoxyviolacein, and (C) provilolacein over time compared to the control without receptor, and the lower part of the figure shows pictures collected after 24 h of incubation. Stars indicate statistical significance as calculated by a one-sided t-test, * $P \leq 0.05$, ** $P \leq 0.01$, *** $P \leq 0.001$, and **** $P \leq 0.0001$. Three strain replicates were used, and negative values were set to zero.

(Chen et al. 2016, Ostrov et al. 2017, Ma et al. 2019, Shi et al. 2019). Meanwhile, only few examples exist of optimization of the violacein pathway towards prodeoxy- and/or proviolacein production in *S. cerevisiae* (Lee et al. 2013, DeLoache et al. 2016, Sanford et al. 2022), where exact titers are reportedly low although exact numbers have not been published (Lee et al. 2013, Li et al. 2018, Zhou et al. 2018). Additional optimization of the violacein pathway by identification of bottlenecks and adjustment of enzyme expression levels in the pathway accordingly may further increase titers (Fang et al. 2015, Ostrov et al. 2017, Ahmed et al. 2021). However, extensive engineering of the strain would remove the advantage of pigments derived from the violacein pathway being easy to implement as sensor outputs.

Finally, to evaluate the applicability of each colorimetric output for dipstick assays in clinical settings, the colorimetric outputs were evaluated on paper slips. Induction was evaluated by drying the respective output strains with and without the receptor onto paper slip and comparing these side-by-side after wetting with media with or without 1 μM α-pheromone. As complex sample solutions such as serum, blood, urine and saliva are often tested in clinical settings, we evaluated this in complex media. We found that the lycopene strains produced a statistically significant output after 6 h of induction ($p = 0.0028$, one-sided unpaired t-test) and after 24 h of induction ($p = 2.6e-05$, one-sided unpaired t-test; Fig. 4A, top). The outputs of the prodeoxyviolacein and proviolacein strains compared to the controls without receptor after 24 h of incubation were statistically significant ($p = 0.0061$ and $p = 0.0012$ for prodeoxy- and proviolacein, respectively, one-sided unpaired t-test; Fig. 4B-C, top). At this time point, both outputs were detectable by the naked eye, but had a lower intensity compared to lycopene (Fig. 4A-C, bottom). Overall, the TOD was shorter for lycopene and the intensity of this pigment was stronger compared to that of prodeoxyviolacein and proviolacein. A summary of the respective pigments and their applicability in different settings is presented in Table 2.

Although direct comparison is made difficult by the use of different fungal ligand-receptor pairs, known to affect sensitivity and dynamic range (Billerbeck et al. 2018, Shaw et al. 2019), our lycopene strain showed a similar performance to those previous reported for this output (Ostrov et al. 2017). The TOD of our strain on slips was 6 h, as compared to the previously reported 8–9 h (Ostrov et al. 2017), while the TOD in liquid culture was 4 h as compared to the previously reported 3 h (Ostrov et al. 2017). Even so, the TOD of the lycopene strain is several times longer compared to that of bioluminescence, with reported TOD of 30 min in liquid solution (Miettinen et al. 2022). Depending on the requirement on the ease-of-use of a test, lycopene may still be preferable as an output, as it does not require additional reagents (Miettinen et al. 2022). Due to there being no need for external machinery to validate the output, applications in non-laboratory environments are possible, such as in remote clinical settings or in industry. However, while prodeoxy- and proviolacein were shown to be applicable in bioengineering settings, these colorimetric outputs did not give a comparable result in liquid or on paper slips.

To summarize, prodeoxy- and proviolacein showed a result comparable to that of lycopene on agar plates, but on both paperslips and in liquid culture the output intensity was lower and the TOD longer. Based on the difference in output intensity between the induction on agar plate versus liquid culture and paper slips indicate that there might be unknown factors affecting the pigment development. Nevertheless, we established that the TOD for these outputs was 24 on paper slips and on agar plates with inducer, while previous studies only reported on the induction on agar plates after 36 h respectively 48 h of incubation (DeLoache

Table 2. Summary for colorimetric used in this study. An overview of the results for each of the colorimetric outputs lycopene, prodeoxyviolacein, and proviolacein, together with a summary of the pathway and pigment properties.

Output	Lycopene	Prodeoxyviolacein	Proviolacein
Output color	Red	Green	Brown/green
Number of pathway genes	5	3	4
Gene(s) induced by the mating pathway	2x *crtI*	*vioE*	*vioE*
Genes in pathway	*crtE, crtB,* 2x *crtI, FAD1*	*vioA, vioB, vioE*	*vioA, vioB, vioC, vioE*
Robust wavelengths (nm)	395, 600	395, 750	395, 750
Sensitive wavelength (nm)	420	450	450
Time to measurable absorbance in liquid culture (h)	4	Non-measurable	Non-measurable
Time to measurable pigment intensity on paper slip (h)	6	24	24

et al. 2016, Rantasalo et al. 2018). Altogether, this work indicates that lycopene remains the preferred colorimetric output for liquid and paper slip applications of YBBs, while prodeoxyviolacein and proviolacein show comparable performance as colorimetric outputs in bioengineering settings.

Acknowledgements

The authors wish to thank Tom Ellis and Will Shaw for providing the minimized pathway Design 4 strain. Thanks to our collaborators Francesca Di Bartolomeo, Simone Balzer Le, and Giang-Son Nguyen at SINTEF for advice and input during this project.

Supplementary data

Supplementary data is available at *FEMSLE Journal* online.

Conflicts of interest: None declared.

Funding

This work was supported by the Joint Programming Initiative on Antimicrobial Resistance (JPIAMR) and The Swedish Research Council for funding of this project [project number 2019-00304].

Data and code availability

Raw data and scripts used in this study are available at https://github.com/AndreaClausenLind/ColorimetricOutputs

Data analysis and visualization All data analysis was performed in R (version 4.0.3) with the tidyverse, janitor, readxl, broom, patchwork, hrbrthemes, minpack.lm, and viridis packages.

References

Adeniran A, Sherer M, Tyo KEJ. Yeast-based biosensors: design and applications. *FEMS Yeast Res* 2015;**15**:1–15.

Ahmed A, Ahmad A, Li R *et al.* Recent advances in synthetic, industrial and biological applications of violacein and its heterologous production. *J Microbiol Biotechnol* 2021;**31**:1465–80.

Bardwell L. A walk-through of the yeast mating pheromone response pathway. *Peptides* 2005;**26**:339–50.

Billerbeck S, Brisbois J, Agmon N *et al.* A scalable peptide-GPCR language for engineering multicellular communication. *Nat Commun* 2018;**9**:1–12.

Chen Y, Xiao W, Wang Y *et al.* Lycopene overproduction in *Saccharomyces cerevisiae* through combining pathway engineering with host engineering. *Microb Cell Fact* 2016;**15**:113.

DeLoache WC, Russ ZN, Dueber JE. Towards repurposing the yeast peroxisome for compartmentalizing heterologous metabolic pathways. *Nat Commun* 2016;**7**:11152.

Esch RK, Wang Y, Errede B. Pheromone-induced degradation of Ste12 contributes to signal attenuation and the specificity of developmental fate. *Eukaryotic Cell* 2006;**5**:2147–60.

Fang M-Y, Zhang C, Yang S *et al.* High crude violacein production from glucose by *Escherichia coli* engineered with interactive control of tryptophan pathway and violacein biosynthetic pathway. *Microb Cell Fact* 2015;**14**:8.

Jarque S, Bittner M, Blaha L *et al.* Yeast biosensors for detection of environmental pollutants: current state and limitations. *Trends Biotechnol* 2016;**34**:408–19.

Kapolka NJ, Taghon GJ, Rowe JB *et al.* DCyFIR: a high-throughput CRISPR platform for multiplexed G protein-coupled receptor profiling and ligand discovery. *Proc Natl Acad Sci USA* 2020;**117**:13117–26.

Kemp HA, Sprague GF. Far3 and five interacting proteins prevent premature recovery from pheromone arrest in the budding yeast *Saccharomyces cerevisiae*. *Mol Cell Biol* 2003;**23**:1750–63.

Lee ME, Aswani A, Han AS *et al.* Expression-level optimization of a multi-enzyme pathway in the absence of a high-throughput assay. *Nucleic Acids Res* 2013;**41**:10668–78.

Li T, Chen X, Cai Y *et al.* Artificial protein scaffold system (AProSS): an efficient method to optimize exogenous metabolic pathways in *Saccharomyces cerevisiae*. *Metab Eng* 2018;**49**:13–20.

Lin H-L, Lin C-C, Lin Y-J *et al.* Revisiting with a relative-density calibration approach the determination of growth rates of microorganisms by use of optical density data from liquid cultures. *Appl Environ Microb* 2010;**76**:1683–5.

Lopreside A, Wan X, Michelini E *et al.* Comprehensive profiling of diverse genetic reporters with application to whole-cell and cell-free biosensors. *Anal Chem* 2019;**91**:15284–92.

Ma T, Shi B, Ye Z *et al.* Lipid engineering combined with systematic metabolic engineering of Saccharomyces cerevisiae for high-yield production of lycopene. *Metab Eng* 2019;**52**:134–42.

Miettinen K, Leelahakorn N, Almeida A *et al.* A GPCR-based yeast biosensor for biomedical, biotechnological, and point-of-use cannabinoid determination. *Nat Commun* 2022;**13**:3664.

Ostrov N, Jimenez M, Billerbeck S *et al.* A modular yeast biosensor for low-cost point-of-care pathogen detection. *Sci Adv* 2017;**3**:e1603221.

Rantasalo A, Kuivanen J, Penttilä M *et al.* Synthetic toolkit for complex genetic circuit engineering in *Saccharomyces cerevisiae*. *ACS Synth Biol* 2018;**7**:1573–87.

Sanford A, Kiriakov S, Khalil AS. A toolkit for precise, multigene control in *Saccharomyces cerevisiae*. *ACS Synth Biol* 2022;**11**:3912–20.

Shaw WM, Yamauchi H, Mead J *et al.* Engineering a model cell for rational tuning of GPCR signaling. *Cell* 2019;**177**:782–96.e27.

Shi B, Ma T, Ye Z *et al.* Systematic metabolic engineering of *Saccharomyces cerevisiae* for lycopene overproduction. *J Agric Food Chem* 2019;**67**:11148–57.

Skrekas C, Ferreira R, David F. Fluorescence-activated cell sorting as a tool for recombinant strain screening. In: Mapelli V, Bettiga M (eds.), *Yeast Metabolic Engineering: Methods and Protocols*. New York, NY: Springer US, 2022, 39–57.

Strickfaden SC, Winters MJ, Ben-Ari G *et al.* A mechanism for cell-cycle regulation of MAP kinase signaling in a yeast differentiation pathway. *Cell* 2007;**128**:519–31.

Wahid E, Ocheja OB, Marsili E *et al.* Biological and technical challenges for implementation of yeast-based biosensors. *Microb Biotechnol* 2023;**16**:54–66.

Zhou Y, Li G, Dong J *et al.* MiYA, an efficient machine-learning workflow in conjunction with the YeastFab assembly strategy for combinatorial optimization of heterologous metabolic pathways in *Saccharomyces cerevisiae*. *Metab Eng* 2018;**47**:294–302.

Received 27 February 2024; **revised** 30 April 2024; **accepted** 22 May 2024